

15. Wallin M et al. *Phys. Rev. B* **49** 12115 (1994)
16. Götze W J. *Phys. C* **12** 1279 (1979)
17. Gold A. *Physica C* **190** 483 (1992)
18. Vollhardt D, Wölfle P. *Phys. Rev. B* **22** 4666 (1980)
19. Belitz D, Gold A, Götze W. *Z. Phys. B* **44** 273 (1981)
20. Fisher M P A. *Phys. Rev. Lett.* **65** 923 (1990)
21. Huang K, Meng H-F. *Phys. Rev. Lett.* **69** 644 (1992)

Mesoscopic phenomena in disordered superconductors

A Frydman, E P Price, R C Dynes

1. Introduction

The superconductor–insulator (SI) transition in 2D ultrathin films has been thoroughly investigated during recent years using two different morphologies; a *uniform* film in which the morphology is homogeneous down to atomic scale [1] and a *granular* film in which the morphology consists of grains of about one hundred angstrom in diameter [2]. In both cases it is found that as the normal-state sheet resistance, R_N , is increased, the superconductivity is weakened and eventually the sample behaves as an insulator. However, the nature of SI transition is very different in the two morphologies. In the uniform case the amplitude of the superconducting gap, Δ , and the critical temperature, T_c , decrease simultaneously as R_N increases (so that $\Delta/T_c = \text{const}$), implying that the magnitude of the superconducting order parameter decays with increasing resistance [1]. In granular films, on the other hand, T_c and Δ remain at bulk values throughout the entire SI transition. In this case the superconducting transition as a function of temperature becomes broader as R_N increases until the sample becomes insulating (see Fig. 2). This behavior implies that in granular films, the individual grains are large enough to support a bulk superconductor order parameter. However, as R_N increases, phase fluctuations appear between the grains and long range phase coherence is destroyed; thus the sample no longer exhibits global superconducting properties [2]. Even though the general mechanism for the SI transition in granular superconductors is understood, the nature of the resistive ‘tail’ on the superconducting side is still a topic of interest as is the detailed role that spatial phase fluctuations play in the destruction of superconductivity. For this reason we have studied samples with sub-micron dimensions that have a relatively small number of grains along the length of the sample. We investigated samples with lengths ranging from 0.1–2 μm and, by applying *in situ* quench-condensation techniques we were able to go through the SI transition using a single sample with only a minor change in its morphology. We present data from samples having different lengths and at different stages of the transition. In all cases, samples which show signs of superconducting behavior exhibit a series of discontinuous voltage jumps in the $I-V$ curves, which we interpret as sequential destructions of dc supercurrents in individual weak links between grains. In addition, these samples are characterized by a rich profile of conductance fluctuations as a function of bias voltage or magnetic field. The amplitude of these fluctuations scales with the sample conductance and may reach values much larger than the normal-metal universal conductance fluctuation value of e^2/h . The latter features are ascribed to interference effects of the superconducting wavefunction within quantum-coherent regions. This interference

is modulated by a magnetic flux penetrating the sample due to an external magnetic field or to self induced flux from the current flowing through the granular system.

2. Experimental

We prepared the samples by thermally evaporating a strip of Pb, connected to four leads, on a Si substrate. Next, we cut a slit in the Pb strip, 0.1–2 μm wide, using e-beam lithography and dry plasma etching. In order to prevent oxidation of the Pb we coated the sample *in situ* with a 20 Å layer of Ag. The sample was then immersed in a cryogenic evaporator which was equipped with a Sn source. We evaporated sequential ultrathin layers of Sn onto the slit in the Pb while the substrate was held at $T = 10$ K, and measured the transport properties after each evaporation stage. This set-up allowed us to change the resistance *in situ* and go through the entire insulator-superconductor transition using a single sample. Figure 1 illustrates the sample geometry and shows an STM picture of a similar quench-condensed film. It is seen that the grain sizes are typically 100 Å in diameter. An estimate based on transport data yields a similar value [3]. We expect, therefore, that our samples consist of about 10–150 grains along the current direction. Standard dc and lock-in based ac methods were used to measure resistance versus temperature ($R-T$), current-voltage ($I-V$), dynamic resistance-voltage ($dV/dI-V$) and magnetoresistance ($R-H$) curves for different R_N . All measurements were performed in an rf shielded room.

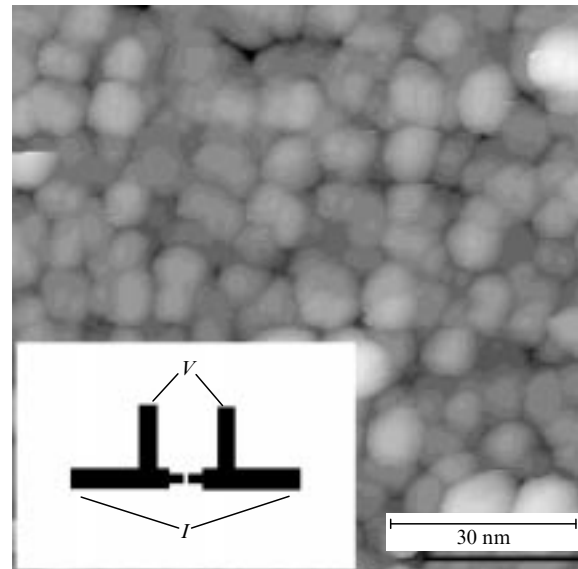


Figure 1. STM scan of a 100 Å film of quench condensed Pb taken at $T = 8$ K. Inset: A schematic representation of the sample.

3. Results

In Figure 2 we show $R-T$ curves for a 1.5 μm long sample. Decreasing R_N corresponds to increasing the film thickness. These curves are similar to those seen in large granular 2D samples [2]. Note that ‘ T_c ’ barely changes throughout the SI transition, while the ‘tails’ of the $R-T$ curves become broader as the normal state resistance is increased. This implies that the destruction of superconductivity is caused by phase fluctuations between the grains rather than by suppression

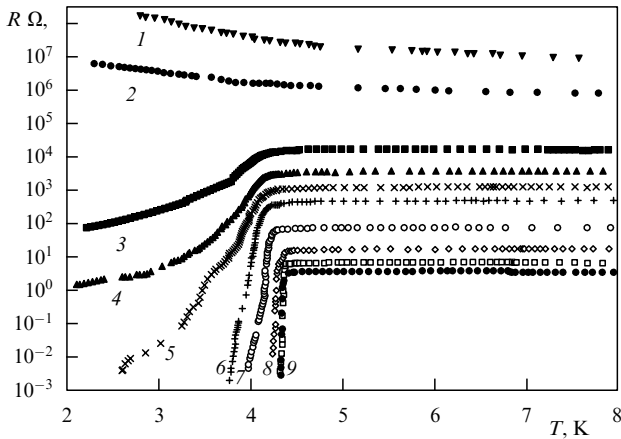


Figure 2. Resistance versus temperature of a 1 μm long sample for different evaporation stages. Curves a-i correspond to an average film thickness of: 53, 55, 56.5, 58, 60, 65, 68, 71 and 75 Å respectively.

of superconductivity within the grains themselves. The $I-V$ curves, on the other hand, are qualitatively different from those observed in large films. While there are no unique features in the current-voltage characteristics when the sample is in the normal state, a number of non-trivial features emerge when the sample shows signs of superconductivity. Figure 3 displays typical $I-V$, $dV/dI-V$ and $R-H$ curves for samples measured deep in the ‘superconducting’ state. It is seen that the $I-V$ is hysteretic and exhibits abrupt voltage jumps. Each one of these jumps is associated with a change in the $I-V$ slope, indicating that the resistance is changing discontinuously. Besides these sharp features there is an additional modulation of the resistance at finite voltage as a function of bias or magnetic field. A close look at the $dV/dI-V$ curve which exhibits both the sharp discontinuities and the resistance fluctuations reveals the following differences between the two types of modulation:

(1) The $I-V$ voltage jumps are hysteretic. Sweeping the current back and forth *past* an individual jump yields different $I-V$ traces. The resistance fluctuations do not exhibit hysteresis. Sweeping the current back and forth between two $I-V$ discontinuities produces the same fluctuation profile.

(2) The resistance fluctuations do not represent a discontinuous resistance change. Rather, the resistance fluctuates around an average background.

(3) An external magnetic field has only a small influence on the sharp discontinuities, acting to shift the resistance jumps to lower bias. Furthermore, a field of H or $-H$ has the same effect on these features. The influence of H on the finer fluctuations is more dramatic, yielding an entirely different fluctuation profile for $H = 0$, 300 Oe or -300 Oe (see Fig. 4).

The conductance fluctuations have much in common with the universal conductance fluctuations frequently seen in mesoscopic normal metals [4]: they are sample specific and appear to be a *fingerprint* of the microscopic configuration of the grains. It turns out, however, that in the disordered superconductor the amplitude of the fluctuations is not universal. In all granular superconductors of length shorter than 2 μm the average size of the conductance fluctuations is 10–15% of the conductance; hence the conductance fluctuations scale with the conductance itself. This was observed for more than 10 samples at different evaporation stages,

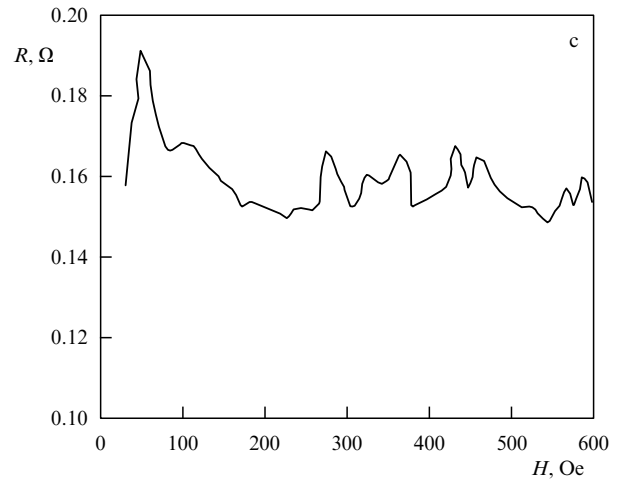
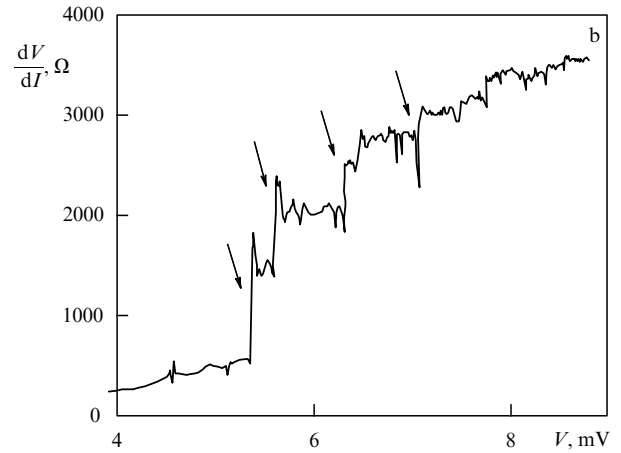
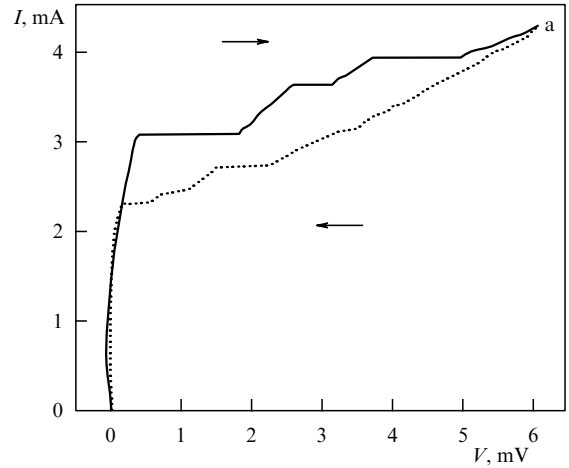


Figure 3. Top: $I-V$ characteristic of a 1 μm sample taken at $T = 2$ K. The heavy line is a sweep up and the light line is a sweep down. Middle: A typical $dV/dI-V$ curve for a 0.1 μm sample. $T = 2$ K. The arrows indicate sharp resistance jumps which correspond to the discontinuities in this sample’s $I-V$ curve. Bottom: Magnetoresistance trace of a 3000 Å sample taken while a $V = 1.2$ mV bias was applied to the sample.

measured at different temperatures and with resistances varying from 10000–0.01 Ω . Since we are able to change the normal-state conductance of a given superconducting sample *in situ* by several orders of magnitude, we have observed conductance fluctuations varying in amplitude from e^2/h to $10^4 \times e^2/h$! This is illustrated in Fig. 5, which depicts $dI/dV-V$ traces for samples with resistance spanning 4 orders of magnitude. Note that despite this vast spread in

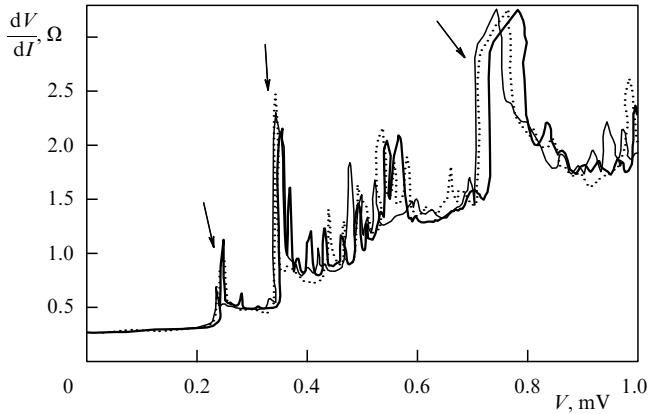


Figure 4. $dV/dI-V$ for a 3000 Å sample taken at $H = 0$ (heavy solid line), $H = 300$ Oe (light solid line) and $H = -300$ Oe (dotted line). The arrows indicate the position of the hysteretic sharp $I-V$ discontinuities.

resistances, the ratio between the fluctuation magnitude and the average conductance value appears to be very similar in all cases. In this regard, the effects we see are clearly different from the mesoscopic behavior seen in normal metals. In the following section we propose a qualitative scenario to explain the origin of these features based on superconductive interference effects in the disordered superconductor.

4. Discussion

We start this section by considering a SQUID circuit which contains two weak links connected by a superconducting loop. It is known that for any type of SQUID, I_c oscillates as a function of the magnetic flux, ϕ , penetrating the loop. The oscillation period is the flux quantum, ϕ_0 , and the amplitude depends on the critical currents of the weak links in the SQUID. If the critical currents of the two weak links are different (an asymmetric SQUID), one arm of the loop carries more current than the other, and therefore application of a bias current introduces self-induced flux in the loop. The supercurrent will oscillate as a function of the external magnetic field or of the current flowing in the circuit, even in the absence of an applied magnetic field. At the high enough current bias the critical current of the links is exceeded, leading to a voltage drop and a finite resistance. At this stage the weak links are in the ac Josephson regime. The phases of the superconductors on both sides are not locked but they are still coherent. Thus, the resistance of the SQUID, measured at finite bias, is also affected by interference of the superconducting wave-function and it oscillates with the same period as the supercurrent.

A superconducting granular film is essentially an array of series and parallel asymmetric SQUID circuits. For any grain configuration, the current will flow in a percolation network through the most strongly coupled grains (see Fig. 6). As increasing current is driven through the sample, the critical current, I_c , of some of the weak links constructing the percolation path is exceeded. A sudden voltage drop occurs across each link which loses its dc supercurrent, leading to a discontinuous increase in the total sample resistance. Since each link is likely to be characterized by a hysteretic $I-V$ (as is common for a Josephson junction), the global $I-V$ exhibits a hysteretic, multiple-switching trace. The resistance of each 'quasi' SQUID loop oscillates as a function of the magnetic

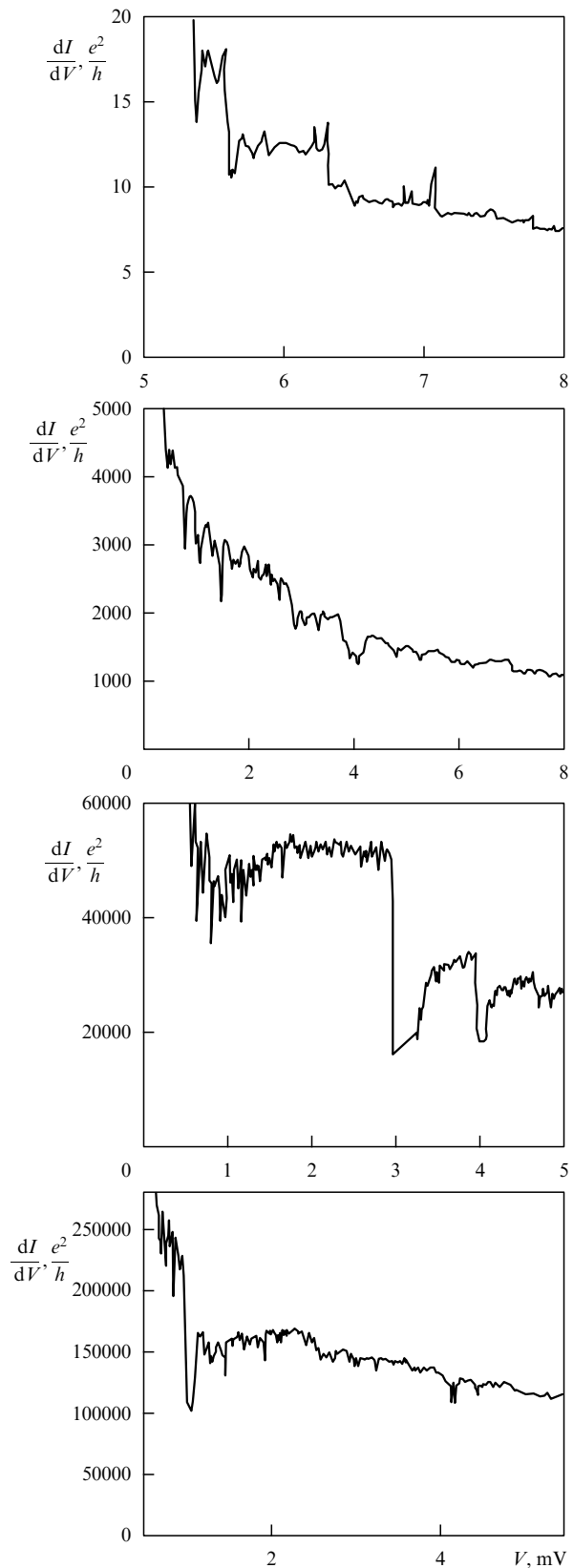


Figure 5. $dV/dI-V$ in units of e^2/h for some representative samples.

field or the current flowing in the sample (inducing flux through the loops). The contribution from all individual oscillations will add up to a measurable fluctuation profile,

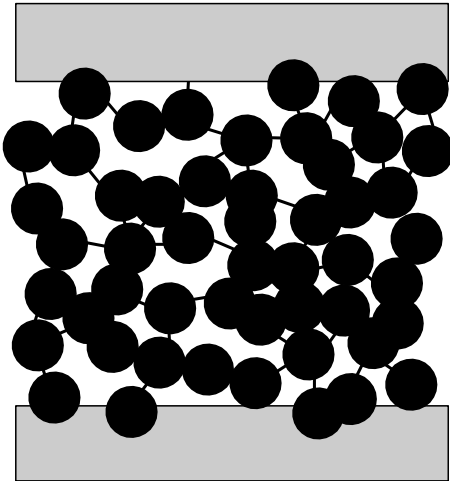


Figure 6. Schematic sketch of the current percolation network through the granular system. The solid line sections represent 'broken' weak links which are connected by 'good' superconducting regions, as indicated by the dotted lines.

as long as the various loops are quantum coherent. It is of interest to note that the relative amplitude of the oscillations (about 10–15% of the conductance) does not change for sample lengths between 1000 Å and a few μm . For samples longer than $10\mu\text{m}$ the fluctuation magnitude decays strongly. It seems reasonable, therefore, to speculate that there is a typical coherence length, a few microns in size, which plays a role similar to L_ϕ in a normal metal.

A small magnetic field can have two types of influence on the I – V curves. Features which stem from exceeding a supercurrent are expected to be slightly shifted to smaller bias values because of the dependence of I_c on H . In addition, H introduces a phase change in each loop, altering any I – V features associated with quantum interference. Hence our notion that the fluctuations stem from interference effects, while the I – V discontinuities represent destruction of dc superconductivity in links is further supported by the dependence of the dV/dI – V curves on the magnetic field as illustrated in Fig. 4. Note that a magnetic field of 300 Oe, while much smaller than H_c of the grains, is larger than the typical field scale for the conductance fluctuations (a few tens of Oe as seen in Fig. 3). Such a field is indeed expected to modify the interference pattern and give rise to a totally different fluctuation trace for both $H = 300$ Oe and $H = -300$ Oe.

5. Conclusion

In summary, we have studied electrical transport properties of mesoscopic granular superconductors. These small structures allow us to focus on the effects of phase fluctuations in the granular system. We observe both discrete stages of the destruction of superconductivity by loss of phase locking between the grains as well as manifestations of superconductive wave-function interference through the disordered film.

Acknowledgment. We gratefully acknowledge fruitful discussions with S I Applebaum, R P Barber, A V Herzog, Y Naveh, M Pollak and P Xiong. This research was supported by AFOSR grant No. f49620-92-j-0070.

References

1. Valles J M, Jr, Dynes R C, Garno J P *Phys. Rev. Lett.* **69** 3567 (1992)
2. Valles J M, Jr, Dynes R C *Mat. Res. Soc. Symp. Proc.* **195** 375 (1990) and references therein; White A E, Dynes R C, Garno J P *Phys. Rev. B* **33** 3549 (1986); Dynes R C et al. *Phys. Rev. Lett.* **53** 2437 (1984)
3. Herzog A V et al. *Phys. Rev. Lett.* **76** 668 (1996); Herzog A V, Xiong P, Dynes R C (to be published)
4. Washburn S, Webb S A *Adv. Physics* **35** 375 (1986); Al'tshuler B L, Lee P A *Physics Today* **41** (12) 36 (1988); Webb R A, Washburn S *Physics Today* **41** (12) 46 (1988)

Low-temperature resistivity of underdoped cuprates

A N Lavrov, V F Gantmakher

In high- T_c cuprates the metallic state is obtained as a result of hole or electron doping of the parent antiferromagnetic insulator. The nature of this insulator–metal transformation has not been sufficiently understood, mainly because of strong electron correlations which crucially complicate the picture of the normal state [1, 2]. The electron correlations obviously play a dominating role in 'undoped', parent compounds, driving these systems into an insulating state. As the doping increases, and the system deviates essentially from half filling, the importance of electron correlations diminishes, and cuprates are generally believed to evolve towards Fermi liquids in the so-called 'overdoped' range. However, an agreement on how one should treat cuprates at intermediate doping, where the high- T_c superconductivity occurs, has not yet been achieved, in spite of very intense studies of strongly-correlated systems in the last 10 years. The main problem is still that little is known about cuprates in the normal state, because of the superconductivity hiding the normal-state properties over a large part of the phase diagram.

Recent experiments by Ando, Boebinger et al. [3, 4] on $\text{La}_{2-x}\text{Sr}_x\text{CuO}_4$ single crystals utilizing magnetic fields up to 61 T to suppress superconductivity have extended measurements of the normal-state resistivity towards low temperatures for the whole range of hole doping. These measurements have revealed rather unusual behavior for the underlying normal state. For all underdoped compositions ($x < 0.16$) both the in-plane and out-of-plane resistivities at low temperatures demonstrated a similar logarithmic increase whenever the resistivity increased or decreased at high temperatures [3, 4]. This logarithmic increase of the resistivity was considered as evidence of the insulating behavior, and the insulator–metal crossover was suggested to take place far in the superconducting region, somewhere near the optimum doping. If the $\log T$ divergence of the low-temperature resistivity were an inherent property of high- T_c cuprates, this would point to a general peculiarity associated with strong electron correlations implying non-Fermi-liquid behavior [5]. Similar investigations performed on $\text{Bi}_2\text{Sr}_2\text{CuO}_y$ crystals [6] have shown, however, that ρ_{ab} may be temperature independent at low T as well as logarithmically divergent, depending on the sample's purity.

It is also possible that the unusual $\log T$ resistivity behavior observed in [3, 4] may be associated with the effect of the strong magnetic field itself rather than with properties of the normal state underlying high- T_c superconductivity.